

Open  
Access

## Dynamic Adsorption of Lead by Novel Graphene Oxide-polyethersulfone Nanocomposite Membrane in Fixed-bed Column

Nik Rashida Nik Abdul Ghani<sup>1</sup>, Mohammed Saedi Jami<sup>1,\*</sup>

<sup>1</sup> Department of Biotechnology Engineering, Kuliyyah of Engineering, International Islamic University Malaysia, 53100 Kuala Lumpur, Malaysia

### ABSTRACT

The existence of a high dosage of heavy metals in industrial effluents represents the greatest challenge in wastewater treatment. Of these heavy metals, lead (Pb) is recognized as a longstanding contaminant due to rapid industrialization in the semiconductor and electronics industries that are harmful to the environment and human health. The development of a modified graphene oxide nanocomposite membrane was sought as a potential adsorbent for the removal of lead ions by continuous adsorption. In this study, graphene oxide-polyethersulfone nanocomposite (GPN) membrane was fabricated via non-solvent induced phase inversion (NIPS) method where the modification of membrane was conducted by incorporating graphene oxide (GO) in the matrix polymer solution. The effect of the dynamic adsorption process was investigated together with the influence of flowrate, initial lead concentration, and bed height. The adsorption was efficient with 10 ml/min of flow rate, 100 ppm of feed concentration, and 0.06 cm of bed height in terms of the elevated adsorption capacity. The experimental adsorption data were evaluated to predict the breakthrough curve of lead adsorption onto the membrane using the Thomas model, the Bohart-Adams model, the Yoon-Nelson model, and the dose-response model. The breakthrough curves were well fitted with the Bohart-Adams model and the maximum adsorption capacity was found to be 1614 mg/g with the initial Pb concentration of 100 ppm at a flow rate of 10 ml/min. The high coefficient of determination (R<sup>2</sup>) and the low sum of squared errors (SSE) on the Bohart-Adams models indicate a good fit of the experimental data for the effect of flowrate, feed concentration and bed height.

#### Keywords:

dynamic adsorption, graphene-oxide,  
nanocomposite membrane,  
breakthrough models

Copyright © 2020 PENERBIT AKADEMIA BARU - All rights reserved

Received: 12 October 2020

Revised: 1 December 2020

Accepted: 24 January 2021

Published: 2 February 2021

## 1. Introduction

Heavy metal pollution is one of the global problems due to rapid industrialization and urbanization. Of these heavy metals, lead (Pb) is one of the common and most toxic pollutants in natural waters. The Pb contaminants are predominantly associated with wastewater effluents from the semiconductor and electronics industries that are harmful to the environment and human health [4]. An effective treatment method to overcome the contaminated wastewater by heavy metal residues remains a great challenge. Common conventional methods that had been utilized to remove heavy metals including Pb from wastewater effluents are chemical precipitation, solvent extraction,

\* Corresponding author.

E-mail address: saedi@iium.edu.my

ion exchange, electrochemical removal, and coagulation. However, these methods have limitations such as inconvenient, large space needed, incomplete removal, high energy consumption low efficiency, generation of toxic sludge, and expensive disposal.

Recent developments in nanotechnology and membrane technology have further increased the effectiveness of adsorbent materials providing innovative systems for improving environmental remediation. Graphene is a nanomaterial with a two-dimensional mesh of carbon atoms arranged in the form of a honeycomb lattice which is the lightest, strongest, thinnest and best heat and electricity conducting material. Significantly, the development of next-generation filtration and separation membranes using graphene-based material has stood up to scrutiny and proved to be efficient in water purification [9]. Graphene oxide (GO), a highly oxidized form of graphene sheet, has been investigated due to easy dispersion in aqueous solution as these oxygen moieties make GO hydrophilic [17]. The GO-based membrane becomes an emerging method in wastewater treatment because of its hydrophilicity, ease of fabrication, strong mechanical stability and industrial scale production [8,10]. Therefore, this study aims to fabricate the asymmetric GO-polyethersulfone nanocomposite (GPN) membrane via a non-soluble induced phase separation (NIPS) method for lead removal. The modification of PES membrane was conducted by incorporating graphene oxide GO in the matrix polymer solution. The produced GPN membrane then was utilized for the dynamic adsorption study. Dynamic adsorption analysis is the best approach to understand the irregular flow patterns and to obtain design models that could be applicable for the commercialization of membrane systems due to the limitation of the batch adsorption system where the treatment of small volume of polluted wastewater and inaccessible authentic data for scale-up [7].

## 2. Materials and Methods

### 2.1 Materials and Chemicals

All reagents used for fabrication were analytical grade. Lead nitrate ( $\text{PbNO}_3$ ; 99%) was purchased from R&M Chemicals. Deionized water was used as the nonsolvent for polymer precipitation and sample preparation. Commercial grade polyethersulfone (PES) (Ultrason E6020P, MW = 75,000 g mol<sup>-1</sup> and glass transition temperature 225 °C) was supplied by BASF, Ludwigshafen, Germany. Polyvinylpyrrolidone (PVP) (MW = 40,000 g mol<sup>-1</sup>) was used as a pore-forming additive for the membrane preparation and N, N- dimethylformamide (DMF, 99.5%) as a solvent, and were all purchased from R&M chemicals, Canada. The synthesized graphene oxide was used throughout the experiment.

### 2.2 Fabrication of GPN membrane

The graphene oxide polymer nanocomposite (GPN) membranes were prepared by the phase inversion method according to Wang *et al.*, [16] with some modifications. Dimethylformamide (DMF) was used as a solvent and deionized water as the non-solvent. Firstly, GO was dispersed in DMF and sonicated for 1 h. Then, PES and polyvinylpyrrolidone (PVP) were added to the above mixture and was stirred at 50 °C for 24 h to obtain a well-dispersed casting solution. Then, the resulting homogenous casting solution was put on an ultrasonic bath and degassed to eliminate air bubbles. Subsequently, the casting solution was poured on a clean glass plate (210 × 297 × 5 mm) to cast the membrane of 200 μm thickness. After 60 seconds of pre-evaporation at room temperature, it was immersed into the non-solvent bath (coagulation bath) and kept in the container for up to 24 h. The prepared membrane was washed with deionized water and then preserved in water before use.

### 2.3 Dynamic adsorption experimental setup

The continuous adsorption of Pb (II) by GPN membrane was conducted according to Zhang *et al.*, [18] with slight modification. The dynamic adsorption process was set up in a stainless-steel cylindrical column with an inner diameter of 2.2 cm and a height of 30 cm. The fibre membranes were cut into a circle shape with an effective membrane area is 3.8 cm<sup>2</sup> before they were placed in the cell holder. A layer of woven wire mesh filter was constructed on each end of the cell to support the membrane, and a perforated filter disc was placed in one end of the cell to prevent leakage. The well-organized cell was then sealed for the solutions to flow through. The schematic of the column set up is shown in Figure 1. The flow rate of the feed solutions was controlled by a peristaltic pump and the solutions were pumped in a down-flow mode. The treated sample at the exit of the column was collected at pre-defined time intervals. The final concentration of Pb in the solution was determined by a spectrophotometer.

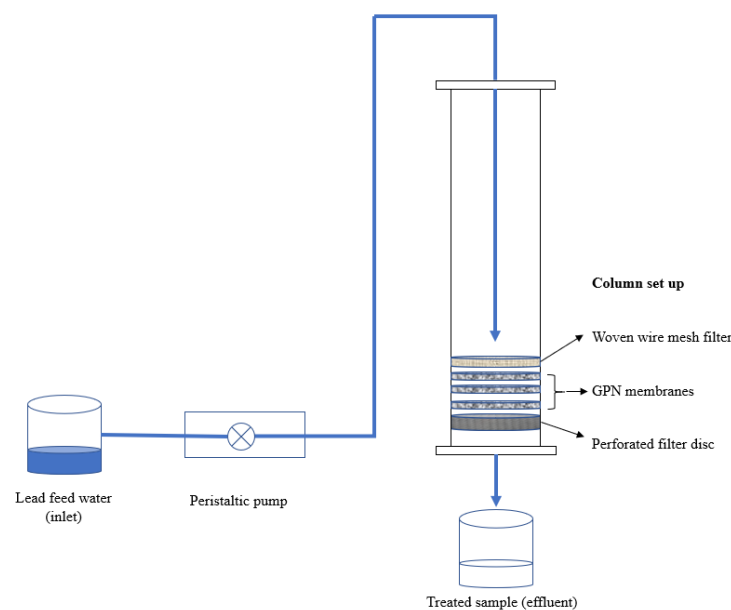


**Fig. 1.** Dynamic adsorption experimental setup for Pb removal

### 2.4 Effect of feed concentration, flow rate, and bed height

To investigate the continuous Pb adsorption on GPN membranes under various conditions, experiments were performed at different initial feed concentrations (100, 200, and 300 ppm), different flow rates (10, 15 and 20 ml/min), and different bed heights (0.02, 0.04, and 0.06 cm). In each experiment, one layer of the membrane was used except in the study of the effect of bed height where multiple layers were used. The initial Pb feed solutions were prepared in deionized water. The pH of the initial feed solutions was adjusted to pH 5.0 ± 0.2 to prevent the formation of lead precipitates. The effluent was collected after a pre-determined time and measured for the residual Pb. The amount of lead (Pb) adsorbed on the membrane ( $q$ , mg/g) was calculated based on Equation 1 below [14]:

$$q = \frac{\int_0^t (C_0 - C_t) Q dt}{X} \quad (1)$$

where  $C_0$  (mg/L) is the initial concentration,  $C_t$  (mg/L) is the effluent concentration at time  $t$  (min),  $Q$  (mL/min) is the flow rate, and  $X$  (mg) is the mass of membranes.  $C_t/C_0 = 0.2$  was defined as the breakthrough point and  $C_t/C_0 = 0.9$  as the saturation point, while  $q_b$  (mg/g) and  $q_s$  (mg/g) refer to the adsorption capacity at breakthrough and saturation points, respectively. Bed utilization efficiency ( $\mathcal{E}$ , %) is defined as the ratio of  $q_b$  to  $q_s$ , where a higher value of bed utilization efficiency signifies a better dynamic adsorption performance.

$$\mathcal{E}\% = \frac{q_b}{q_s} \quad (2)$$

### 3. Results and Discussion

#### 3.1 Effect of feed concentration

Basically, changes in feed concentration affects the shape of the breakthrough curves [13]. In this study, different Pb feed concentrations (100, 200 and 300 ppm) were investigated at a constant flow rate of 10 ml/min and 0.02 cm bed height. The breakthrough in columns with high feed concentrations was reached much earlier (50 min for 300 ppm and 80 min for 200 ppm) compared to the low feed concentration (100 min for 100 ppm), as shown in Figure 2. In terms of the adsorption capacity, at the breakthrough point, the Pb adsorption capacity for 100, 200 and 300 ppm were 7215, 12152 and 7408 mg/g, respectively while at the saturation point the Pb adsorption capacity was 967, 4348 and 1252 mg/g, respectively. The adsorption capacity at 200 ppm is slightly higher due to the lower concentration difference between initial and final concentration. However, the dynamic adsorption performance was better for lower concentration feed solution where the bed utilization efficiency for 100, 200 and 300 ppm were 74, 27 and 59 %, respectively.

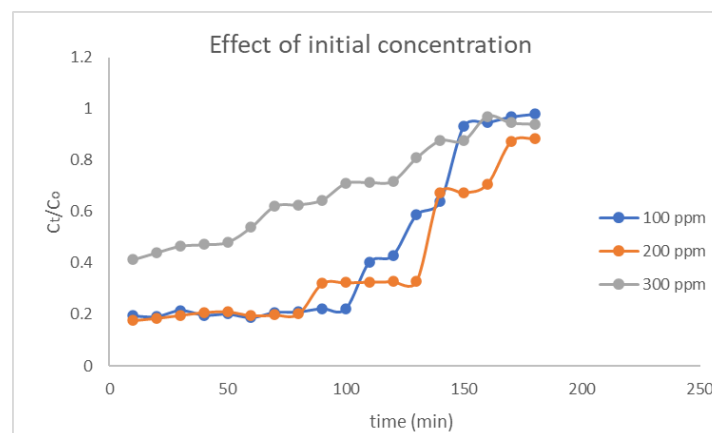


Fig. 2. Effect of initial feed concentration on breakthrough curves:  $C_t/C_0$  vs time

#### 3.2 Effect of flow rate

The effect of flow rate on the breakthrough curve of Pb adsorption by GPN membrane is shown in Figure 3. The slopes of the curves became steeper when the flow rate increased from 10 to 20 mL/min. This result revealed that at a higher flow rate, the time required to reach the breakthrough and saturation point is decreased. This phenomenon occurred due to the residence time of Pb solution in the column or on the GPN membrane was reduced, leading to an earlier breakthrough time when the flow rate increased [18]. The Pb adsorption capacity on GPN membranes is inversely proportional to the flow rate. The values of adsorption capacity decreased from 7215 to 476 mg/g and from 1047 to 590 mg/g at the breakthrough point and saturation point, respectively. In terms of

bed utilization efficiency, the results showed 68, 64 and 8% for flow rates 10, 15 and 20 ml/min, correspondingly. Therefore, a lower flow rate and longer contact time were optimal for Pb removal due to higher adsorption capacity and higher bed utilization efficiency.

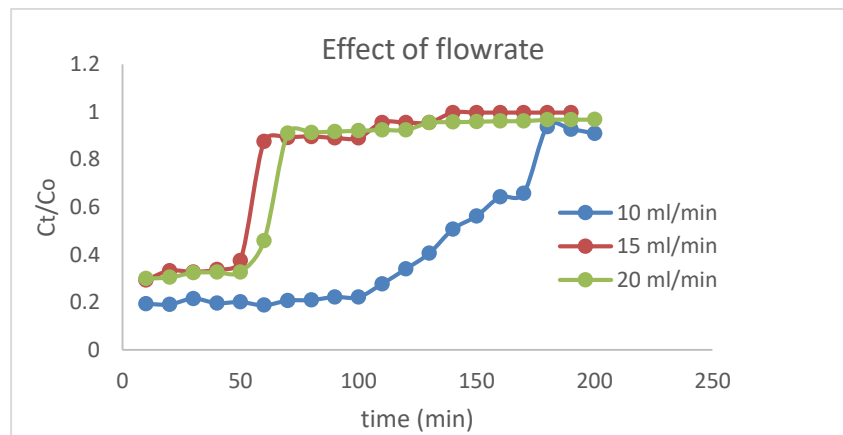


Fig. 3. Effect of the flow rate of Pb adsorption on breakthrough curves:  $C_t/C_0$  vs time

### 3.3 Effect of bed height

The effect of bed height on breakthrough curves was studied at a constant flow rate of 10 ml/min and a constant initial feed concentration of 200 ppm and the result is illustrated in Figure 4. The breakthrough curves shifted to the right and prolonged the breakthrough point at high bed height. Experimentally, 1, 2 and 3 layers of GPN membranes were positioned in the fixed-bed column equivalent to a bed height of 0.02, 0.04 and 0.06 cm, respectively. The adsorption capacity at the breakthrough point was elevated from 227 to 8617 mg/g when the bed height is increased as well as the adsorption capacity at the saturation point. This result describes that the more available active sites for adsorption at the higher bed height due to an increase in the membrane active area [3]. The summary of the adsorption capacity at the breakthrough and saturation point as well as bed utilization efficiency were presented in Table 1.

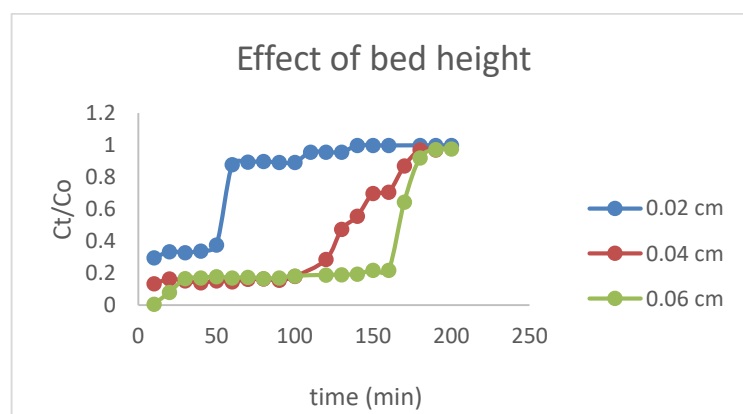


Fig. 4. Effect of bed height of Pb adsorption on breakthrough curves:  $C_t/C_0$  vs time

**Table 1**

Adsorption capacity and bed utilization efficiency for each effect of parameters

<b>Feed concentration</b>	<b>100ppm</b>	<b>200 ppm</b>	<b>300 ppm</b>
$q_b$ (mg/g)	7215.238	12152.38	7408.571
$q_s$ (mg/g)	967.5714	4348.571	1252.571
$\mathcal{E}$ (%)	74.5	27.9	59.1
<b>Flow rate</b>	<b>10 ml/min</b>	<b>15 ml/min</b>	<b>20 ml/min</b>
$q_b$ (mg/g)	7215.238	5941.905	476.1905
$q_s$ (mg/g)	1047.429	927.1429	590
$\mathcal{E}$ (%)	68.8	64	8
<b>Bed height</b>	<b>0.02 cm</b>	<b>0.04 cm</b>	<b>0.06 cm</b>
$q_b$ (mg/g)	227.619	5909.143	8617.143
$q_s$ (mg/g)	74.66667	1056	1024.19
$\mathcal{E}$ (%)	30.4	55.9	84.1

### 3.4 Modelling of breakthrough curves

The experimental continuous adsorption data were modelled to provide mathematical and quantitative approaches in designing a column adsorption process successfully. In this work, three models, namely the Thomas model, the Bohart-Adams model and the Yoon-Nelson model, have been used to predict the breakthrough curves of Pb adsorption onto the GPN membranes. These three models were commonly utilized in the determination of breakthrough curves for the adsorption of organic compounds and inorganic ions in a fixed-bed column [1,11,18]. The Thomas model is mainly assuming the Langmuir isotherm and follows second-order reversible reaction kinetics, where it is specifically suitable to estimate the adsorption process in which external and internal diffusion is not the rate-limiting step [5,12]. The Bohart-Adams model assumes the non-instantaneous equilibrium and therefore, the adsorption rate is directly proportional to the adsorbate concentration and the adsorbent residual capacity [2,15]. The Yoon-Nelson model is a simple theoretical model where it is assumed that the probability of adsorbate molecule is related to the adsorbate breakthrough and its adsorption process [6,17].

The non-linear fittings of the experimental data were performed in Microsoft Excel solver (Microsoft 365). The breakthrough curves for all three parametric effects are shown in Figure 5 (a-c). The parameters and values of all three models were tabulated in Table 1. The fitting curves for optimal parameters of 100 ppm of feed concentration, 10 ml/min of flow rate and 0.06 cm of bed height are shown in Figures 5, 6 and 7 while the model equations and parameters are listed in Table 1. Notably that the fittings of Thomas and Yoon-nelson models are overlapped with each other due to the same mathematical equation form of these two models in spite of different model parameters.

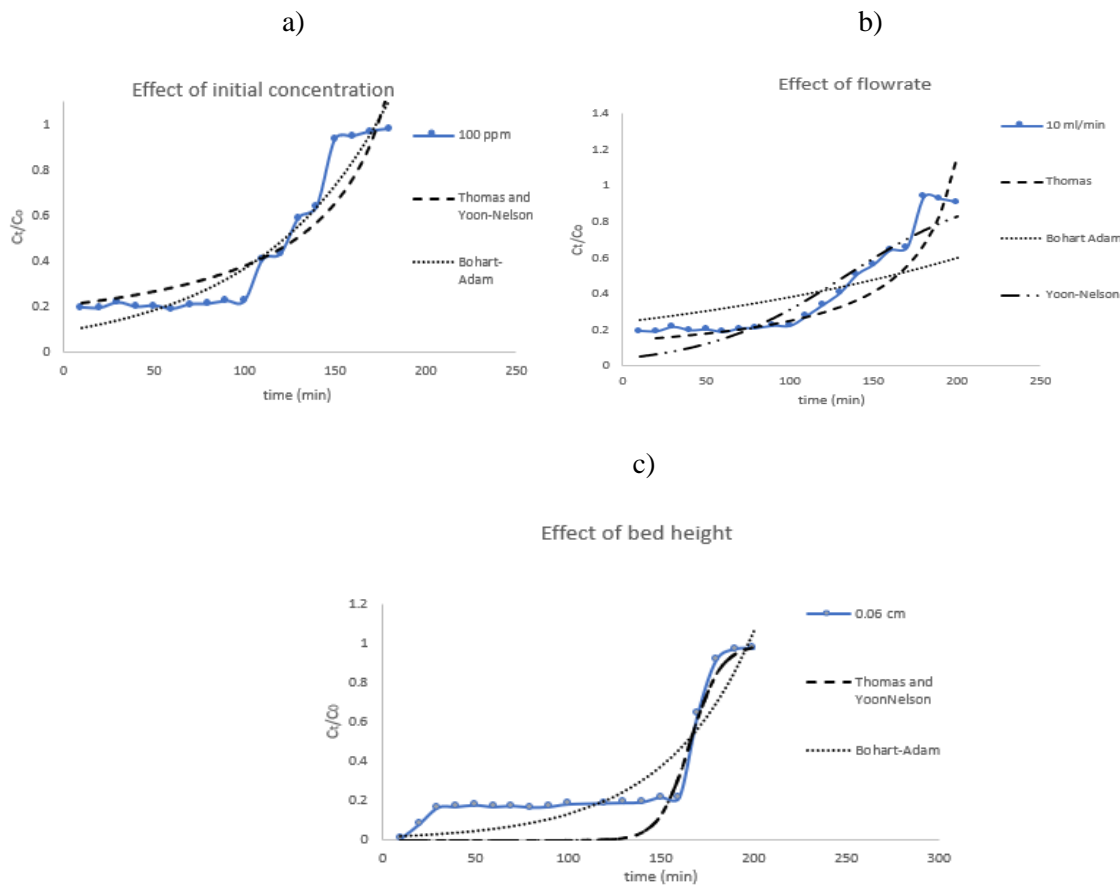


**Fig. 5.** Non-linear fittings of breakthrough curves using the Thomas, Yoon-Nelson and Bohart-Adams models

A good fit of the experimental data to the breakthrough models is demonstrated by the high coefficient of determination ( $R^2$ ) and low sum of squared errors (SSE). In this present study, the  $R^2$  of the Bohart-Adams model was higher than other two models and the SSE of  $C_t/C_0$  of the Bohart-Adams model was much lower than those of the Thomas and Yoon-Nelson models. Therefore, this Bohart Adams model was found to be well-fitted in predicting the dynamic adsorption of Pb on GPN membrane indicating that the adsorption rate is proportional to the residual capacity of the adsorbent and the concentration of the adsorbate. Then, the experiments were done on the optimum parameters condition of 100 ppm of initial Pb feed concentration, 10 ml/min of flow rate and 0.06 cm of bed height with maximum adsorption capacity of 1614 mg/g.

#### 4. Conclusion

In conclusion, The GPN membrane demonstrated good comparative properties to the commercial membrane in terms of adsorption capacity and removal efficiency. It is therefore believed that embedment of GO and PVP to modify the polyethersulfone membrane is an excellent approach to develop high performance membrane and enhance selectivity, and stability of the membrane. The utilization of the GPN membrane in the wastewater treatment can be assessed in further studies of filtration behaviour towards the removal of other contaminants. The development of the GPN membrane would be the best alternative to revolutionize wastewater treatment and beneficial for making this technology accessible to Malaysia.

## References

- [1] Bhaumik, Madhumita, Katlego Setshedi, Arjun Maity, and Maurice S. Onyango. "Chromium (VI) removal from water using fixed bed column of polypyrrole/Fe<sub>3</sub>O<sub>4</sub> nanocomposite." *Separation and Purification Technology* 110 (2013): 11-19.
- [2] Bohart, G. S., and E. Q. Adams. "Some aspects of the behavior of charcoal with respect to chlorine." *Journal of the American Chemical Society* 42, no. 3 (1920): 523-544.
- [3] Ji, Fei, Chaolin Li, Jialin Xu, and Peng Liu. "Dynamic adsorption of Cu (II) from aqueous solution by zeolite/cellulose acetate blend fiber in fixed-bed." *Colloids and Surfaces A: Physicochemical and Engineering Aspects* 434 (2013): 88-94.
- [4] Krause, A., Zimmermann, K. F., & Chowdhury, S. (2015). 2014\_meyer\_estrin\_GSJ-subsidiary-strategy.pdf. 9400.
- [5] Kumar, Dhananjay, Lalit K. Pandey, and J. P. Gaur. "Metal sorption by algal biomass: From batch to continuous system." *Algal Research* 18 (2016): 95-109.
- [6] Kutty, S. R. M., N. M. Y. Almahbashi, A. A. M. Nazrin, M. A. Malek, A. Noor, L. Baloo, and A. A. S. Ghaleb. "Adsorption kinetics of colour removal from palm oil mill effluent using wastewater sludge carbon in column studies." *Heliyon* 5, no. 10 (2019): e02439.
- [7] Manirethan, Vishnu, Niharika Gupta, Raj Mohan Balakrishnan, and Keyur Raval. "Batch and continuous studies on the removal of heavy metals from aqueous solution using biosynthesised melanin-coated PVDF membranes." *Environmental Science and Pollution Research* (2019): 1-15.
- [8] Mkhoyan, K. Andre, Alexander W. Contryman, John Silcox, Derek A. Stewart, Goki Eda, Cecilia Mattevi, Steve Miller, and Manish Chhowalla. "Atomic and electronic structure of graphene-oxide." *Nano letters* 9, no. 3 (2009): 1058-1063.
- [9] Naushad, Mu, ed. *A new generation material graphene: applications in water technology*. Cham: Springer International Publishing, 2019.
- [10] Peng, Weijun, Hongqiang Li, Yanyan Liu, and Shaoxian Song. "A review on heavy metal ions adsorption from water by graphene oxide and its composites." *Journal of Molecular Liquids* 230 (2017): 496-504.
- [11] Perendija, Jovana, Zlate S. Veličković, Ilija Cvijetić, Jelena D. Rusmirović, Vukašin Ugrinović, Aleksandar D. Marinković, and Antonije Onjia. "Batch and column adsorption of cations, oxyanions and dyes on a magnetite modified cellulose-based membrane." *Cellulose* 27, no. 14 (2020): 8215-8235.
- [12] Thomas, Henry C. "Heterogeneous ion exchange in a flowing system." *Journal of the American Chemical Society* 66, no. 10 (1944): 1664-1666.
- [13] Tsai, Wan-Chi, Mark Daniel G. De Luna, Hanna Lee P. Bermillo-Arriegas, Cybelle M. Futralan, James I. Colades, and Meng-Wei Wan. "Competitive fixed-bed adsorption of Pb (II), Cu (II), and Ni (II) from aqueous solution using chitosan-coated bentonite." *International Journal of Polymer Science* 2016 (2016).
- [14] van Elteren, Johannes T., Miha Grilc, Michael P. Beeston, Milagros Santacatalina Reig, and Irena Grgić. "An integrated experimental-modeling approach to study the acid leaching behavior of lead from sub-micrometer lead silicate glass particles." *Journal of hazardous materials* 262 (2013): 240-249.
- [15] Vijayalakshmi, K., B. Mahalakshmi Devi, Srinivasan Latha, Thandapani Gomathi, P. N. Sudha, Jayachandran Venkatesan, and Sukumaran Anil. "Batch adsorption and desorption studies on the removal of lead (II) from aqueous solution using nanochitosan/sodium alginate/microcrystalline cellulose beads." *International journal of biological macromolecules* 104 (2017): 1483-1494.
- [16] Wang, Xiao, Miao Feng, Yan Liu, Huining Deng, and Jun Lu. "Fabrication of graphene oxide blended polyethersulfone membranes via phase inversion assisted by electric field for improved separation and antifouling performance." *Journal of Membrane Science* 577 (2019): 41-50.
- [17] Yoon, Young Hee, and JAMES H. NELSON. "Application of gas adsorption kinetics I. A theoretical model for respirator cartridge service life." *American Industrial Hygiene Association Journal* 45, no. 8 (1984): 509-516.
- [18] Zhang, Shujuan, Qiantao Shi, Christos Christodoulatos, George Korfiatis, and Xiaoguang Meng. "Adsorptive filtration of lead by electrospun PVA/PAA nanofiber membranes in a fixed-bed column." *Chemical Engineering Journal* 370 (2019): 1262-1273.

**Table 2**

Breakthrough models and model parameters based on non-linear regressions for Pb adsorption on GPN membranes

Model	Model formula	Linearized expression	Parameter	Effect of initial concentration	Effect of bed height	Effect of flow rate
Thomas <sup>a</sup>	$\frac{C_t}{C_o} = \frac{1}{1 + e^{\frac{k_T q_0 X}{Q} - k_T C_o t}}$	$\ln\left(\frac{C_o}{C_t} - 1\right) = \frac{k_T q_0 X}{Q} - k_T C_o t$	Theoretical	5790.2	31571.2	5500
			$q_0$ (mg/g)			
			$k_T$ (mL/min.mg)	$2.23 \times 10^{-4}$	$6.09 \times 10^{-4}$	$3.14 \times 10^{-4}$
			$R^2$	0.9515	0.9832	0.9319
			SSE	0.2373	0.3458	0.2778
Bohart-Adams <sup>b</sup>	$\frac{C_t}{C_o} = e^{k_{BA} C_o t - \frac{k_{BA} N_o Z}{u}}$	$\ln\left(\frac{C_o}{C_t}\right) = k_{BA} C_o t - \frac{k_{BA} N_o Z}{u}$	$N_o$ (mg/L)	60250	143327	$10.9 \times 10^4$
			$k_{BA}$ (L/mg.min)	$1.4 \times 10^{-4}$	$1.0 \times 10^{-4}$	$4.54 \times 10^{-5}$
			$R^2$	0.9987	0.9997	0.9867
			SSE	0.1292	0.2873	0.5714
Yoon-Nelson <sup>c</sup>	$\frac{C_t}{C_o} = \frac{1}{1 + e^{k_{YN}(\tau - t)}}$	$\ln\left(\frac{C_o}{C_t} - 1\right) = k_{YN} \tau - k_{YN} t$	$k_{YN}$ ( $\text{min}^{-1}$ )	0.05	0.1218	0.0237
			$\tau$ (min)	70	165	133.08
			$R^2$	0.9515	0.9832	0.9645
			SSE	0.2373	0.3458	0.1678

Note: <sup>a</sup> $k_T$  (mL/(min mg)), Thomas rate constant, and  $q_0$  (mg/g), predicted adsorption capacity; <sup>b</sup> $k_{BA}$  (L/(mg min)), Bohart-Adams kinetics constant,  $N_o$  (mg/L), maximum volumetric adsorption capacity,  $\mu$  (cm/min), linear velocity of the fluid, and  $Z$  (cm), bed height; <sup>c</sup> $k_{YN}$  ( $\text{min}^{-1}$ ), Yoon and Nelson's rate constant, and  $\tau$  (min), time required for 50% breakthrough